engineering proceedings

MDPI

Proceeding Paper

Optimized Electrode Configurations for Multi-Parameter Detection in Microfluidic Impedance Cytometry †

Shengzhi Ji, Huancheng Zhang, Zhiyang Hu and Tieying Xu *

School of Microelectronics, Shanghai University, Shanghai 200444, China; 3289488410@shu.edu.cn (S.J.); huanchengzhang@shu.edu.cn (H.Z.); huzhiyang@shu.edu.cn (Z.H.)

* Correspondence: tieying_xu@shu.edu.cn; Tel.: +33-7829-78228

† Presented at the 12th International Electronic Conference on Sensors and Applications (ECSA-12), 12–14 November 2025; Available online: https://sciforum.net/event/ECSA-12.

Abstract

Microfluidic impedance cytometry enables label-free and real-time single-cell analysis by detecting changes in electrical impedance as cells traverse microchannels. Electrode configuration plays a critical role in determining detection sensitivity, signal quality, and spatial resolution. In this study, finite element simulations were conducted to model the impedance response of mammalian red blood cells under various electrode designs, including coplanar, parallel, tilted, and parabolic configurations, as well as electrode layouts coupled with flow velocity. A multiphysics simulation model is established to analyze the effects of geometric parameters on electric field distribution and impedance response. The results demonstrate that optimized electrode arrangements significantly enhance detection performance and enable multi-parameter analysis. Furthermore, the influence of flow dynamics and dielectric properties on impedance signals is explored. These findings provide both theoretical and experimental guidance for the development of high-efficiency, integrated impedance cytometry platforms, contributing to the advancement of microfluidic systems in biomedical diagnostics and single-cell characterization.

Keywords: microfluidics; impedance detection; electrode configuration

Academic Editor(s): Name

Published: date

Citation: Ji, S.; Zhang, H.; Hu, Z.; Xu, T. Optimized Electrode Configurations for Multi-Parameter Detection in Microfluidic Impedance Cytometry. *Eng. Proc.* **2025**, *volume number*, x. https://doi.org/10.3390/xxxxx

1. Introduction

The pathological state of cells plays a critical role in the early diagnosis and treatment of various diseases, including cancer, infectious diseases, and immune disorders. Conventional pathological diagnosis methods, such as tissue biopsy and microscopic analysis, often require invasive procedures, complicated sample preparation, and manual operation. These limitations highlight the increasing demand for label-free, non-invasive, and high-throughput cell detection technologies in modern biomedical applications.

Microfluidic impedance cytometry (MIC) has emerged as a promising solution, offering significant advantages such as label-free detection, real-time analysis, and single-cell resolution [1]. By leveraging the intrinsic electrical properties of cells, MIC enables sensitive detection and characterization of biological samples without the need for chemical markers. Recent reviews highlight advancements in device integration and real-time analytics for cell characterization [2]. Its integration with microfluidic platforms further enhances throughput, making it suitable for rapid screening applications [3].

However, despite its advantages, the practical performance of MIC systems heavily depends on the design and configuration of the detection electrodes. Various electrode configurations and microchannel designs have been explored to enhance sensitivity and detection efficiency [4]. Traditional coplanar electrode layouts are favored for their simple fabrication but often suffer from non-uniform electric field distribution, resulting in low detection sensitivity and strong dependence on the cell's lateral position within the microchannel [5]. On the other hand, parallel electrode designs offer improved electric field uniformity and signal response but introduce fabrication complexity due to the need for precise alignment.

Electrode placement and channel geometry significantly influence impedance signal characteristics and detection accuracy [6]**.** However, conventional electrode structures are typically optimized for single-parameter detection, such as cell size or membrane capacitance, limiting their ability to capture multidimensional information like lateral position or mechanical properties [7]. This constraint hinders the comprehensive analysis of heterogeneous cell populations, which is increasingly important in applications such as cancer diagnostics and personalized medicine [8].

To address these challenges, this study proposes a series of optimized electrode configurations for microfluidic impedance cytometry. We systematically analyze the performance of coplanar, parallel, tilted, and multi-electrode designs using multiphysics simulation. By evaluating their impact on electric field distribution, impedance response, and detection sensitivity, we aim to establish a framework for multi-parameter cell characterization. Our approach not only improves the detection of cell size and position but also enables indirect assessment of cell mechanical properties, offering new insights for microfluidic diagnostic platforms.

2. Methods

2.1. The Principle of Microfluidic Impedance Detection

2.1.1. Single-Cell Model

Maxwell's mixture theory provides a theoretical basis for analyzing the dielectric properties of cells suspended in a conductive medium. According to this theory, a cell immersed in a conductive solution can be modeled as a dielectric particle. The effective complex permittivity of the cell suspension system—composed of the suspended cells and the surrounding conductive medium—is primarily influenced by three factors: the complex permittivity of the cells, the complex permittivity of the suspending medium, and the volume fraction of the cells within the microfluidic channel. This relationship is expressed by Equation (1).

$$\boldsymbol{\varepsilon^*_{mix}} = \boldsymbol{\varepsilon^*_{me}} \frac{\mathbf{2(1-\varphi)+(1+2\varphi)}\,\frac{\boldsymbol{\varepsilon^*_c}}{\boldsymbol{\varepsilon^*_{me}}}}{\mathbf{(2+\varphi)+(1-\varphi)}\,\frac{\boldsymbol{\varepsilon^*_c}}{\boldsymbol{\varepsilon^*_{me}}}} \quad (1)$$

In this equation, $\boldsymbol{\varepsilon^*_{mix}}$ represents the effective complex permittivity of the cell suspension, $\boldsymbol{\varepsilon^*_{me}}$ denotes the complex permittivity of the suspending medium, $\boldsymbol{\varepsilon^*_c}$ corresponds to the complex permittivity of the cells, and $\boldsymbol{\varphi}$ is the volume fraction of the cells.

Due to the phospholipid bilayer structure of the cell membrane, cells possess the ability to store and release electrical charge when exposed to an electric field, thereby exhibiting capacitive behavior. In contrast, the cytoplasm contains a high concentration of ions and molecules, which results in low resistance to current flow, manifesting primarily as a resistive effect. Therefore, based on the established framework in single-cell electroanalysis, an equivalent circuit model for single cells and the characterization of dielectric properties were defined [9]. At appropriate frequency, the cell can be modeled as an equivalent electrical circuit, as illustrated in Figure 1 [10].

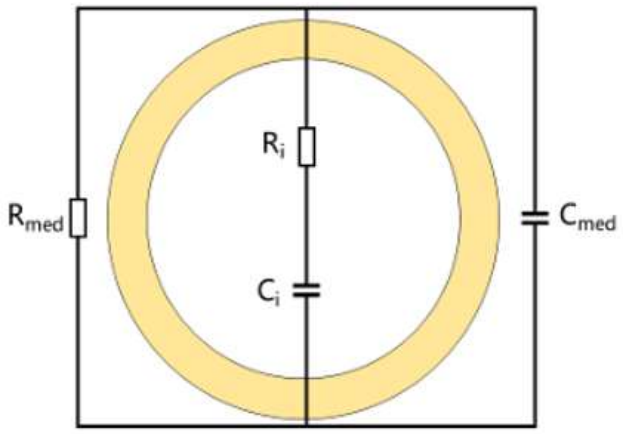

Figure 1. Cell equivalent circuit model. Here, C_{med} and R_{med} represent the capacitance and resistance of the suspension medium, while C_i and R_i represent the capacitance and resistance of the cells.

2.1.2. Principle of Impedance Detection

The principle of microfluidic impedance cytometry is based on monitoring the variation in electrical impedance when a single cell passes through an electric field within a microchannel. As a cell suspended in a conductive medium flow through the detection zone, it perturbs the local electric field due to its distinct dielectric properties compared to the surrounding medium. This perturbation leads to a measurable change in the electrical impedance. The total impedance Z_{total} at the detection region is jointly determined by the impedance of the cell Z_{cell} and the impedance of the suspending medium Z_{med}.

The complex impedance of the cell Z_{cell} is typically influenced by both the membrane capacitance C_{mem} and the cytoplasmic resistance R_c, and can be expressed as Equation (2).

$$Z_{cell} = \frac{1}{j\omega C_{mem}} + R_c \quad (2)$$

where $\omega = 2\pi f$ is the angular frequency of the applied alternating current signal.

Moreover, the total impedance Z_{total} is related to the effective complex permittivity ε^*_{mix} of the suspension containing both the cells and the conductive medium, as described by Equation (3).

$$Z_{cell} = \frac{1}{j\omega \varepsilon^*_{mix} G} \quad (3)$$

where G is the geometric correction factor, which is used to correct the effects of edge fields and non-uniform electric fields.

The impedance variation ΔZ is associated with cell size, membrane integrity, and internal conductivity, making it a valuable parameter for label-free single-cell analysis. By applying multi-frequency excitation, different cellular components and their dielectric properties can be characterized, enabling multi-parameter detection within a single measurement cycle.

2.2. Multiphysics Simulation Platform

To investigate the impact of electrode configurations on impedance detection, a multiphysics simulation model was established using COMSOL Multiphysics software. This platform enables the coupling of electric field and fluid flow, allowing accurate analysis of the interaction between cells, electrodes, and microchannel environments. This platform employs finite element analysis to assess the electric field distribution under

different electrode geometries [11]. The simulation domain includes the microchannel geometry, electrode placement, cell models, and surrounding fluid medium.

Modeling steps include geometry creation, material property assignment, boundary condition setup, and meshing. The microchannel is modeled as a rectangular channel of length 100–120 μm, width 10–20 μm, and height 10–15 μm. The surrounding fluid is assumed to be a conductive electrolyte with conductivity of 1.44 S/m and a relative permittivity of 78.5 [12].

The simulation applies a low-frequency AC signal (typically 100 kHz) at the excitation electrode, with grounding or floating boundary conditions set at other electrodes depending on the configuration. Mesh refinement is concentrated near the electrode edges and the cell surface to ensure solution convergence.

2.3. Electrode Configuration Design

2.3.1. Coplanar and Parallel Electrode Designs

We analyzed two baseline electrode configurations: coplanar electrodes and parallel electrodes, as shown in Figure 2. Coplanar electrodes are patterned on the bottom surface of the microchannel using photolithography, creating an asymmetric electric field distribution. This configuration simplifies fabrication but exhibits poor field uniformity, making impedance signals highly sensitive to cell position [13]. Parallel electrodes are fabricated on opposing surfaces of the channel (top and bottom), yielding a uniform electric field between the electrodes. This design enhances signal sensitivity and reduces positional dependency, albeit at the cost of more complex fabrication processes [14].

Simulation results revealed that parallel electrodes provide a more homogeneous electric field and stronger impedance response compared to coplanar layouts.

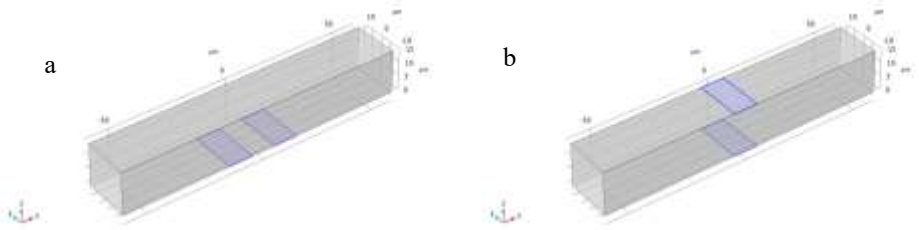

Figure 2. (**a**) Coplanar electrode configuration. (**b**) Parallel electrode configuration.

2.3.2. Tilted Electrode for Lateral Position Detection

To acquire information on the lateral position of cells, a tilted electrode structure was designed, as shown in Figure 3a. In this configuration, the electrodes on the bottom of the channel are tilted relative to the flow direction, while the counter electrodes on the top remain parallel. This asymmetric layout causes the impedance signal peak to shift based on the lateral position of the cell [15]. This tilt introduces a spatial variation in the electric field, enabling position-resolved detection without relying on complex external focusing mechanisms.

However, in practical microfluidic channels, the velocity profile is not uniform but exhibits a spatial gradient. Specifically, it manifests as a parabolic decrease in velocity from the maximum at the center towards zero at the channel walls. Therefore, electrode design for characterizing lateral cell position must account not only for positional differences but also for the associated velocity differences at various lateral positions. Based on the parabolic fluid velocity distribution, parabolic-shaped electrodes were designed as shown in Figure 3b, with the opening of the electrode parabola-oriented opposite to the fluid velocity direction. Consequently, the electrode spacing is smaller where the fluid

velocity is higher, and larger where the fluid velocity is lower. This design ensures that impedance signals from cells at different lateral positions exhibit significant temporal differences.

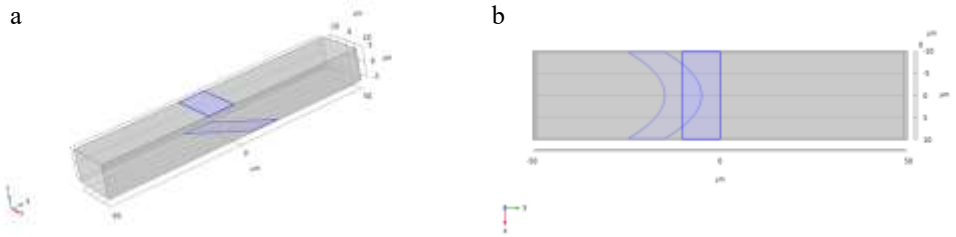

Figure 3. Schematic of tilted electrode design. (**a**) Inclined electrode configuration. (**b**) "Parabolic" electrode configuration that couples fluid velocities.

2.3.3. Multi-Electrode Configuration for Mechanical Property Sensing

For advanced characterization, a multi-electrode configuration was proposed, as shown in Figure 4. By placing electrode pairs upstream and downstream within the channel, the transit time of a cell between electrode pairs can be measured. This transit time correlates with cell deformability and mechanical stiffness, as deformed cells tend to move differently in laminar flow conditions [16]. The combination of spatial localization and mechanical property assessment enhances the multi-parameter detection capability of the system.

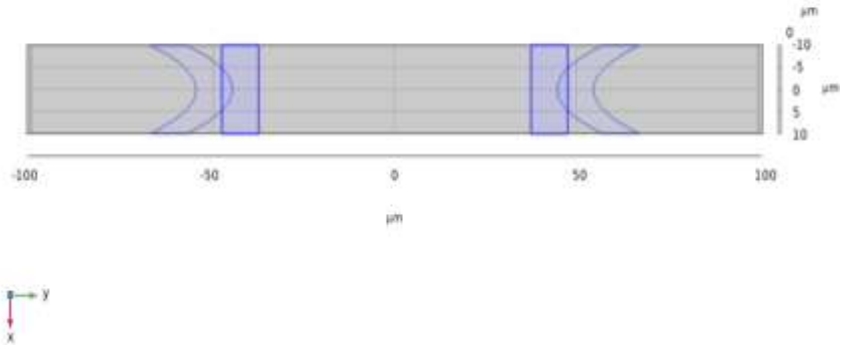

Figure 4. Schematic of multi-electrode layout in microchannel.

2.4. Cell Modeling and Simulation Parameters

In this study, single cells with an average radius of 4 μm, comparable to mammalian red blood cells, were modeled in the microfluidic channel. Cells are modeled as spherical or ellipsoidal particles with a dielectric membrane layer representing the phospholipid bilayer [17]. The core cell body is assigned conductivity of 1 S/m and relative permittivity of 80, while the membrane is set with a much lower conductivity (10^{-5} S/m) and permittivity of 60. The dielectric and electrical parameters of cells were set according to established single-cell impedance characterization methods [18]. All the simulation parameters are shown in Table 1. Simulation conditions include: Cell diameter variations (to analyze size sensitivity); Lateral position changes (for position detection); Transit time measurement (for mechanical analysis)

The applied AC signal frequency is scanned between 1 kHz and 10 MHz to determine the optimal operating condition for impedance detection [19].

Table 1. The parameters used in the simulation process.

Parameters	Values
Cytoplasmic conductivity	1 S/m
Cytoplasmic relative dielectric constant	80
Cell membrane conductivity	10^{-5} S/m
Cell membrane relative dielectric constant	60
Cell radius	4 μm
Suspension medium conductivity	1.44 S/m
Suspension medium relative dielectric constant	78.5
Electrode width	10 μm
AC signal frequency	10^5 Hz

3. Results and Discussion

3.1. Electric Field Distribution and Impedance Response

Simulation results reveal significant differences in electric field distribution between the coplanar and parallel electrode configurations. In the coplanar electrode layout, the electric field lines are primarily confined to the vicinity of the electrode edges at the bottom of the channel, as illustrated in Figure 5a. This results in a highly non-uniform electric field distribution across the channel cross-section. Since electric field lines are always perpendicular to equipotential lines, the concentration of electric field lines near the channel bottom under the coplanar configuration is evident from the equipotential line distribution shown in Figure 5c. Consequently, the longitudinal position of cells passing through significantly affects the impedance signal, thereby reducing detection reliability.

In contrast, the parallel electrode configuration provides a more uniform and symmetric electric field distribution within the detection region, as shown in Figure 5b,d. This configuration consequently yields more stable impedance signals and enhances sensitivity to variations in cell size and properties.

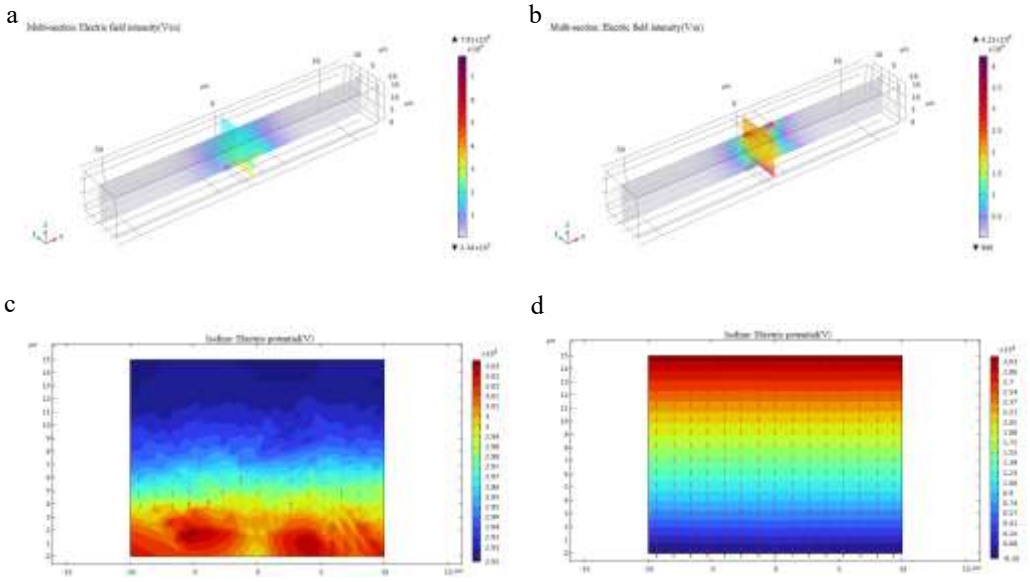

Figure 5. Electric field distribution under different electrode configurations. (**a**) Electric potential distribution with coplanar electrodes. (**b**) Electric potential distribution with parallel electrodes. (**c**) The distribution of equipotential lines of coplanar electrodes. (**d**) The distribution of equipotential lines of parallel electrodes.

Impedance magnitude comparisons from the simulation results further corroborate these findings. Under identical simulation conditions, the impedance change generated by the parallel electrode layout when a cell passes through the electrode region (Figure 6a) is significantly higher than that produced by the coplanar electrode layout (Figure 6b). This confirms the superior detection capability of the parallel electrode layout for cellular impedance sensing applications.

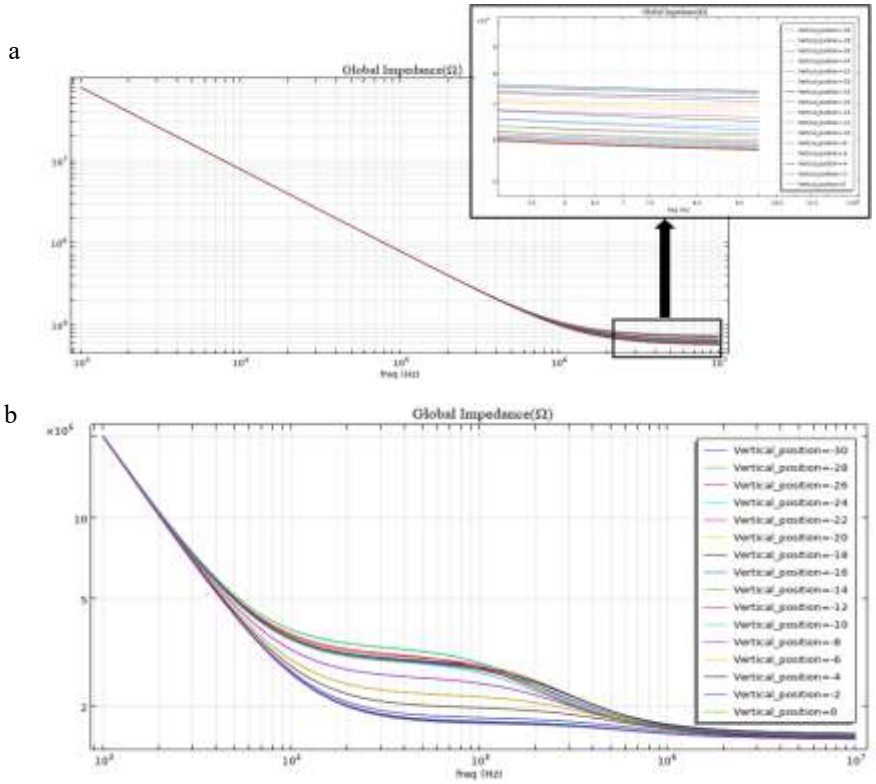

Figure 6. Impedance amplitude response comparison. (**a**) Impedance signal of coplanar electrode configuration. (**b**) Impedance signal of parallel electrode configuration. In both Figure 6a,b, there is a parameter called "Vertical position", with the unit being micrometers. This parameter represents the longitudinal position of the cell along the extension direction of the microfluidic channel.

3.2. Tilted Electrodes for Lateral Position Detection

To enhance the electrode system's capability for detecting the lateral position of cells during transit, thereby enabling the extraction of additional cellular parameters, tilted electrodes were introduced. By orienting the excitation electrodes at a defined angle relative to the channel axis, this design disrupts the symmetry and uniformity of the electric field distribution within the channel. Consequently, the electric field lines are no longer vertical or horizontal but instead traverse the entire flow channel at an angle, forming an "oblique electric field path" in space. As shown in the Figure 7a, the cells on the left side of the channel were exposed to the main electric field lines earlier, while the cells on the right side entered the strong electric field region later. This implies that the position of the impedance peak will shift depending on the lateral position of the cell.

Simulation results in Figure 7b demonstrate a linear correlation between the lateral offset of the cell and the corresponding position of the impedance signal peak. This enables the direct extraction of lateral position information from impedance measurements without the need for additional optical systems.

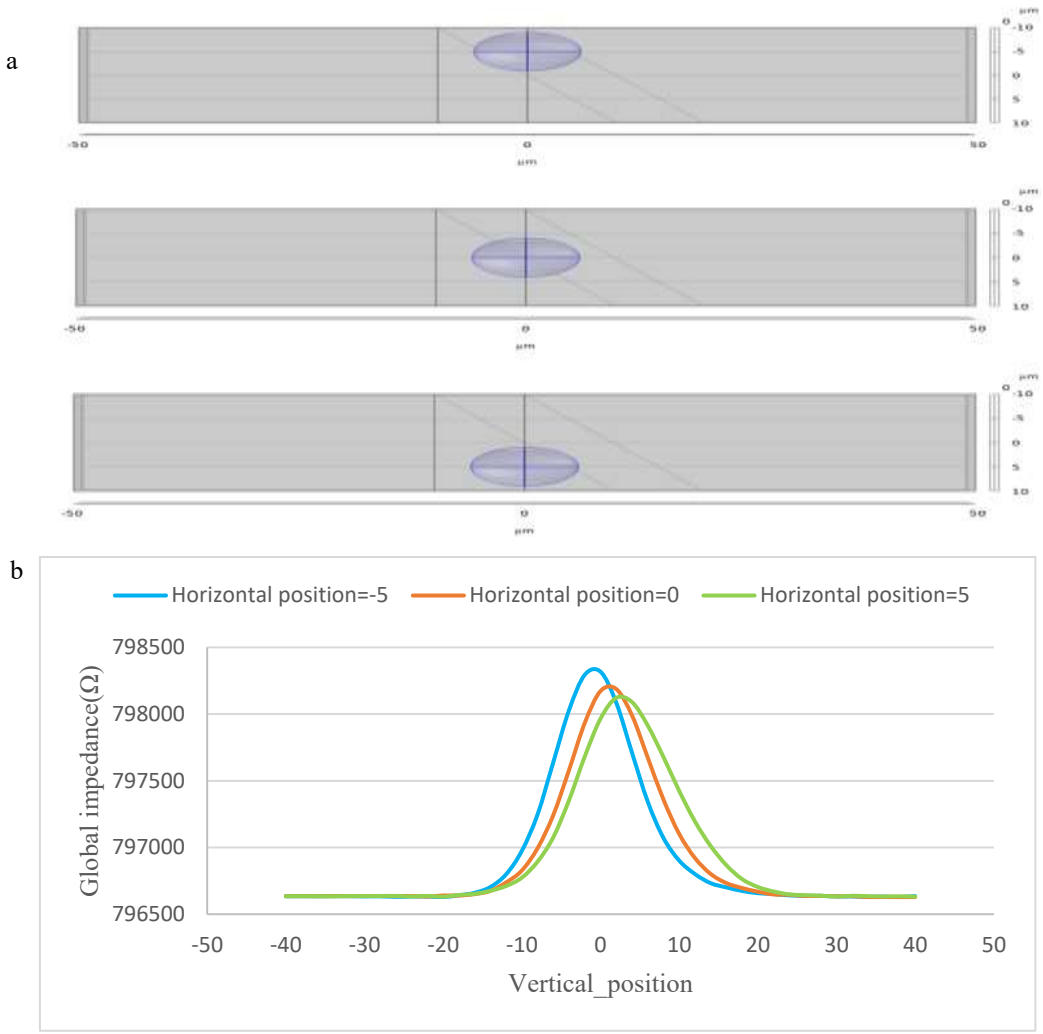

Figure 7. (**a**) The distribution of cells at different lateral positions within the microfluidic channel. (**b**) The relationship between the lateral position of cells in microfluidic channels and the impedance peak shift. Here, the frequency of the transmitted signal is 10^5 Hz.

This method effectively expands the functionality of impedance cytometry from single-parameter to multi-parameter detection, providing valuable insights into cell positioning within microfluidic flows.

3.3. Multi-Electrode Configuration for Mechanical Property Characterization

Further simulations explored the potential of multiple electrode pairs for indirectly characterizing the mechanical properties of cells. By incorporating an additional pair of "parabolic-shaped electrodes" along the flow direction, the mechanical properties of cells can be indirectly extracted by measuring their transit time between detection intervals. Experimental studies using constriction-based deformability cytometry have demonstrated that rigid (fixed) cells exhibit significantly longer transit times compared to deformable cells. For instance, fixed BA/F3 cells—rendered rigid via paraformaldehyde treatment—showed a 2.5-fold increase in the 75th percentile of transit time (1.05 s vs. 0.41 s) relative to untreated controls. Conversely, HL-60 cells treated with Cytochalasin D (increasing deformability) displayed reduced transit times (5.12 s vs. 3.43 s) [20]. Similar trends were observed in MCF-7 model cells using impedance-based constriction systems, where transit time metrics served as quantitative indicators of mechanical phenotype [21]. Previous studies have demonstrated that electrical impedance parameters such as transit

time and amplitude are strongly correlated with red blood cell deformability and pathological status [22].

Simulation results (Figure 8) indicate that by adding a pair of electrodes based on the "parabolic-shaped electrodes" coupled with the fluid velocity profile, the following detection objective can be achieved through dual-parameter detection (lateral position and transit time): cells of the same type located at different lateral positions will exhibit different transit times between the two electrode pairs. Consequently, if cells of different types located at the *same* lateral position exhibit a difference in the time delay between their impedance signals, it can be discerned that these two cell types possess different mechanical properties. Therefore, this design effectively enables the identification of anomalous cells among those passing through the channel.

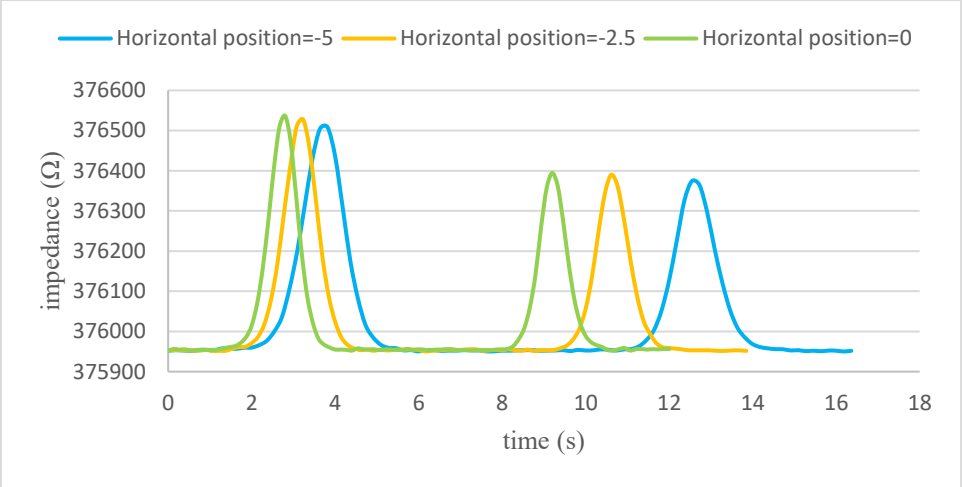

Figure 8. Impedance signals of cells with different mechanical properties.

3.4. Summary of Simulation Results

The simulation results validate the performance advantages of the proposed electrode designs: Parallel electrodes enhance impedance signal stability and sensitivity. Tilted electrodes enable lateral position detection based on impedance signal shift. Multi-electrode configurations provide a feasible method for assessing mechanical properties through transit time analysis.

These findings demonstrate that optimized electrode designs can significantly improve the detection capabilities of microfluidic impedance cytometry systems, supporting their application in multi-parameter single-cell analysis. Moreover, the adaptability of electrode configurations facilitated diverse applications in single-cell analysis [23].

4. Conclusions

Microfluidic impedance cytometry (MIC) provides a portable, label-free, and real-time solution for single-cell analysis, enabling quantitative characterization of cell size, membrane capacitance, cytoplasmic resistance, and dielectric properties. In this study, various electrode configurations—including coplanar, parallel, tilted, and multi-parabolic layouts—were systematically investigated through finite element simulations on the COMSOL platform. The optimized multi-parabolic electrode design positioned upstream and downstream of the microchannel significantly enhanced detection sensitivity, spatial resolution, and multi-parametric detection capability. Moreover, the multi-electrode configuration enabled extraction of mechanical parameters such as cell deformability and stiffness through transit time analysis. This work offers both theoretical foundation and practical guidance for the development of compact, integrated, and high-throughput

impedance cytometry devices, with promising applications in large-scale single-cell characterization and the advancement of personalized diagnostic and therapeutic strategies.

Author Contributions: Conceptualization, S.J., H.Z., Z.H. and T.X.; software, S.J.; investigation, S.J.; writing—original draft preparation, S.J.; writing—review and editing, T.X. and H.Z.; supervision, T.X. All authors have read and agreed to the published version of the manuscript.

Funding: Not applicable.

Institutional Review Board Statement: Not applicable.

Informed Consent Statement: Not applicable.

Data Availability Statement: Not applicable.

Acknowledgments: This project is supported by National Center for Translational Medicine (Shanghai) Shanghai University Branch under the general program (Ref. SUITM-202414).

Conflicts of Interest: The authors declare no conflict of interest.

References

1. Manz, A.; Graber, N.; Widmer, H.M. Miniaturized Total Chemical Analysis Systems: A Novel Concept for Chemical Sensing. *Sens. Actuators B Chem.* **1990**, *1*, 244–248. https://doi.org/10.1016/0925-4005(90)80209-I.
2. Chen, Y.; Guo, K.; Jiang, L.; Zhu, S.; Ni, Z.; Xiang, N. Microfluidic Deformability Cytometry: A Review. *Talanta* **2023**, *251*, 123815. https://doi.org/10.1016/j.talanta.2022.123815.
3. McDonald, J.C.; Whitesides, G.M. Poly(Dimethylsiloxane) as a Material for Fabricating Microfluidic Devices. *Acc. Chem. Res.* **2002**, *35*, 491–499. https://doi.org/10.1021/ar010110q.
4. Cottet, J.; Kehren, A.; van Lintel, H.; Buret, F.; Frénéa-Robin, M.; Renaud, P. How to Improve the Sensitivity of Coplanar Electrodes and Microchannel Design in Electrical Impedance Flow Cytometry: A Study. *Microfluid. Nanofluid.* **2019**, *23*, 11. https://doi.org/10.1007/s10404-018-2178-6.
5. De Ninno, A.; Errico, V.; Bertani, F.R.; Businaro, L.; Bisegna, P.; Caselli, F. Coplanar Electrode Microfluidic Chip Enabling Accurate Sheathless Impedance Cytometry. *Lab Chip* **2017**, *17*, 1158–1166. https://doi.org/10.1039/c6lc01516f.
6. Fang, Q.; Feng, Y.; Zhu, J.; Huang, L.; Wang, W. Floating-Electrode-Enabled Impedance Cytometry for Single-Cell 3D Localization. *Anal. Chem.* **2023**, *95*, 6374–6382. https://doi.org/10.1021/acs.analchem.2c05822.
7. Squires, T.M.; Quake, S.R. Microfluidics: Fluid Physics at the Nanoliter Scale. *Rev. Mod. Phys.* **2005**, *77*, 977–1026. https://doi.org/10.1103/RevModPhys.77.977.
8. Chen, J.; Zheng, Y.; Tan, Q.; Shojaei-Baghini, E.; Zhang, Y.L.; Li, J.; Prasad, P.; You, L.; Wu, X.Y.; Sun, Y. Classification of Cell Types Using a Microfluidic Device for Mechanical and Electrical Measurement on Single Cells. *Lab Chip* **2011**, *11*, 3174–3181. https://doi.org/10.1039/c1lc20473d.
9. Français, O.; Le Pioufle, B. Single Cell Electrical Characterization Techniques. In *Handbook of Electroporation*; Miklavcic, D., Ed.; Springer: Cham, Switzerland, 2016; pp. 1–38. https://doi.org/10.1007/978-3-319-26779-1_15-1.
10. Sun, T.; Green, N.G.; Morgan, H. Analytical and Numerical Modeling Methods for Impedance Analysis of Single Cells On-Chip. *Nano* **2008**, *3*, 55–63. https://doi.org/10.1142/S1793292008000800.
11. Cheng, X.; Liu, Y.S.; Irimia, D.; Demirci, U.; Yang, L.; Zamir, L.; Rodríguez, W.R.; Toner, M.; Bashir, R. Cell Detection and Counting through Cell Lysate Impedance Spectroscopy in Microfluidic Devices. *Lab Chip* **2007**, *7*, 746–755. https://doi.org/10.1039/b705082h.
12. Ahuja, K.; Rather, G.M.; Lin, Z.; Sui, J.; Xie, P.; Le, T.; Bertino, J.R.; Javanmard, M. Toward Point-of-Care Assessment of Patient Response: A Portable Tool for Rapidly Assessing Cancer Drug Efficacy Using Multifrequency Impedance Cytometry and Supervised Machine Learning. *Microsyst. Nanoeng.* **2019**, *5*, 34. https://doi.org/10.1038/s41378-019-0073-2.
13. Zhu, S.; Zhang, X.; Zhou, Z.; Han, Y.; Xiang, N.; Ni, Z. Microfluidic Impedance Cytometry for Single-Cell Sensing: Review on Electrode Configurations. *Talanta* **2021**, *233*, 122571. https://doi.org/10.1016/j.talanta.2021.122571.
14. McGrath, J.S.; Honrado, C.; Moore, J.H.; Adair, S.J.; Varhue, W.B.; Salahi, A.; Farmehini, V.; Goudreau, B.J.; Nagdas, S.; Blais, E.M.; et al. Electrophysiology-Based Stratification of Pancreatic Tumorigenicity by Label-Free Single-Cell Impedance Cytometry. *Anal. Chim. Acta* **2020**, *1101*, 90–98. https://doi.org/10.1016/j.aca.2019.12.033.

15. Yang, D.; Ai, Y. Microfluidic Impedance Cytometry Device with N-Shaped Electrodes for Lateral Position Measurement of Single Cells/Particles. *Lab Chip* **2019**, *19*, 3609–3617. https://doi.org/10.1039/c9lc00819e.
16. Caselli, F.; De Ninno, A.; Reale, R.; Businaro, L.; Bisegna, P. A Bayesian Approach for Coincidence Resolution in Microfluidic Impedance Cytometry. *IEEE Trans. Biomed. Eng.* **2021**, *68*, 340–349. https://doi.org/10.1109/TBME.2020.2995364.
17. Asami, K. Characterization of Heterogeneous Systems by Dielectric Spectroscopy. *Prog. Polym. Sci.* **2002**, *27*, 1617–1659. https://doi.org/10.1016/S0079-6700(02)00015-1.
18. Cheung, K.; Gawad, S.; Renaud, P. Impedance Spectroscopy Flow Cytometry: On-Chip Label-Free Cell Differentiation. *Cytometry Part A* **2005**, *65*, 124–132. https://doi.org/10.1002/cyto.a.20141.
19. Sun, T.; Morgan, H. Single-Cell Microfluidic Impedance Cytometry: A Review. *Microfluid. Nanofluidics* **2010**, *8*, 423–443. https://doi.org/10.1007/s10404-010-0580-9.
20. Apichitsopa, N.; Jaffe, A.; Voldman, J. Multiparameter Cell-Tracking Intrinsic Cytometry for Single-Cell Characterization. *Lab Chip* **2018**, *18*, 1430–1439. https://doi.org/10.1039/C8LC00240A.
21. Chen, J.; Zheng, Y.; Tan, Q.; Shojaei-Baghini, E.; Zhang, Y.L.; Li, J.; Prasad, P.; You, L.; Wu, X.Y.; Sun, Y. Classification of Cell Types Using a Microfluidic Device for Mechanical and Electrical Measurement on Single Cells. *Lab Chip* **2011**, *11*, 3174–3181. https://doi.org/10.1039/C1LC20473D.
22. Xu, T.; Lizarralde-Iragorri, M.A.; Roman, J.; Ghasemi, R.; Lefèvre, J.-P.; Martincic, E.; Brousse, V.; Français, O.; El Nemer, W.; Le Pioufle, B. Characterization of Red Blood Cell Microcirculatory Parameters Using a Bioimpedance Microfluidic Device. *Sci. Rep.* **2020**, *10*, 9869. https://doi.org/10.1038/s41598-020-66693-4.
23. Zhu, J.; Pan, S.; Chai, H.; Zhao, P.; Feng, Y.; Cheng, Z.; Zhang, S.; Wang, W. Microfluidic Impedance Cytometry Enabled One-Step Sample Preparation for Efficient Single-Cell Mass Spectrometry. *Small* **2024**, *20*, 2310700. https://doi.org/10.1002/smll.202310700.